Phytopathology Research

A potential biocontrol agent *Streptomyces tauricus* XF for managing wheat stripe rust

Ruimin Jia[†], Keyu Xiao[†], Ligang Yu, Jing Chen, Lifang Hu and Yang Wang[*]

Abstract

Wheat stripe rust, caused by *Puccinia striiformis* f. sp. *tritici* (*Pst*), is a devastating disease threatening global wheat production. Biocontrol by beneficial microorganisms is considered an alternative to synthetic fungicide applications. This study aimed to investigate the mechanisms involved in the biocontrol of wheat stripe rust by streptomycetes. A streptomycete strain XF, isolated from the rhizospheric soil of peony, was identified as *Streptomyces tauricus* based on morphological characteristics and phylogenetic analysis. We determined the inhibitory effect of XF on *Pst* and biocontrol effect on the disease using XF fermentation filtrate (FL) and actinomycete cell suspension (AC). Results revealed that FL inhibited urediniospore germination by up to 99% and rendered a lethality rate of 61.47% against urediniospores. Additionally, crude extract of ethyl acetate phase of FL caused cytoplasm releases from urediniospores and the deformation of germ tubes. Furthermore, histochemical analyses revealed that treatments of plants with AC and FL increased reactive oxygen species, inhibited haustorium formation, and reduced the biomass of *Pst* in leaves. Electron microscopy showed that XF mycelium was able to colonize the leaf surface. Moreover, gene expression assays revealed that AC and FL treatments induced the expression of a number of pathogenesis-related genes in wheat leaves. Besides, in the greenhouse experiments, the control effects of AC and FL reached 65.48% and 68.25%, respectively. In the field, application of XF fermentation broth significantly reduced the disease indices of stripe rust by 53.83%. These findings suggest that XF is a potential biocontrol agent for managing wheat stripe rust disease.

Keywords *Puccinia striiformis* f. sp. *tritici*, *Streptomyces tauricus*, Wheat stripe rust, Biological control, Antagonism, Induced systematic resistance

Background

Wheat stripe rust caused by the obligate parasitic fungus *Puccinia striiformis* f. sp. *tritici* (*Pst*) is a devastating foliar disease that has historically caused significant yield losses worldwide. It has become the greatest biotic constraint to wheat production in the twenty-first century, resulting in annual losses of one billion dollars worldwide (Beddow et al. 2015; Schwessinger 2017). China is the largest wheat producer and is the largest stripe rust endemic region in the world (Ye et al. 2019). China's epidemiological pattern of stripe rust is more complex and variable than in other countries, making disease control more difficult (Ye et al. 2019). To effectively manage wheat stripe rust, an integrated control strategy must be adopted based on planting disease-resistant cultivars, supplemented by fungicides and cultivation management measures. However, most significant genetically resistant varieties gradually lose their resistance after 3 to 6 years of field cultivation due to the rapid *Pst* virulence mutations (Han et al. 2015). Additionally, the continual and indiscriminate use of fungicides causes environmental pollution and the development of more aggressive isolates as they acquire resistance against routinely used fungicides

[†]Ruimin Jia and Keyu Xiao contributed equally to this work.

*Correspondence:
Yang Wang
wangyang2006@nwsuaf.edu.cn
College of Plant Protection, Northwest A & F University, Yangling 712100, Shaanxi, China

Jia *et al. Phytopathology Research*   (2023) 5:14

Page 2 of 16

(Lucas et al. 2015). Therefore, there is an urgent need to develop new strategies for better disease control.

In the recent era of biologically sustainable agriculture, biocontrol agents (BCAs) for preventing crop diseases are receiving considerable attention, and BCAs have emerged as a promising measure for management of wheat stripe rust. For example, *Cladosporium cladosporioids* and *Alternaria alternate* inhibit urediniospore germination via parasitism (Zhan et al. 2014; Zheng et al. 2017). *Bacillus subtilis* E1R-j has been shown to effectively control wheat stripe rust by causing urediniospores and germ tubes to rupture, releasing protoplasm, and causing fungal structures to malfunction (Li et al. 2013). Endophytic *Paneibacillus xylanexedens* 7A and *B. megaterium* 6A induce wheat resistance and reduce the disease severity of stripe rust with efficacy of 61.11% and 65.16%, respectively (Kiani et al. 2021). Recent studies reveal that *Streptomyces* spp. have excellent biological control efficacy against various wheat fungal pathogens. *S. pratensis* S10 was reported to significantly inhibit the growth of *Fusarium graminearum* and effectively control wheat scab and decrease deoxynivalenol content (Zhang et al. 2021). Two BCAs, *S. neyagawaensis* and *S. viridosporus*, decrease the severity of wheat leaf rust and the number of pustules (Sub et al. 2004; Araujo et al. 2019). In a greenhouse pot trial, plants treated with seed coatings of either *S. hygroscopicus* or *S. lydicus* had > 24% lower disease severity than control plants infected with *F. pseudograminearum* (O'Sullivan et al. 2021). Several *Streptomyces* spp. members have been recognized as diazotrophic endophytes that protect wheat against *Rhizoctonia solani* attack by direct antagonism and induction of plant defenses (Patel et al. 2018).

Streptomycetes can suppress or kill microbial opponents by producing bioactive molecules, such as enzymes disrupting fungal cell walls and compounds with fungicidal activity (Gupta et al. 1995; Diaz-Cruz et al. 2022). Biocontrol activity often occurs before the pathogens completely infect their respective hosts. It has been shown that foliar sprays of bioactive compounds produced by *Streptomyces* spp. can prevent symptoms caused by microbial pathogens, although *Streptomyces* spp. inhabiting plant leaves are rare (Han et al. 2021). Additionally, *Streptomyces* spp. have been shown to trigger localized and systemic resistance in plants and to inhibit pathogen growth via induction of plant defense mechanisms (Lehr et al. 2008). In general, induced resistance can be divided into systemic acquired resistance (SAR) and induced systemic resistance (ISR). The induction of plant defenses by *Streptomyces* species differs from traditional ISR, as it involves features of both ISR and SAR, as well as cross-talk between many different phytohormone signaling pathways (Newitt et al. 2019). In

any case, the ability of *Streptomyces* spp. to act as inducers of systemic plant resistance renders them promising candidates for effective biocontrol of plant diseases.

However, so far, there are few reports regarding the utilization of *Streptomyces* spp. for controlling wheat stripe rust. In this study, *S. tauricus* strain XF was screened as a potential BCA and displayed high antagonistic activity against *Pst*. This study aims to define further the biocontrol abilities of XF against wheat rust to advance the development of new biological fungicides.

Results

Streptomyces isolate XF suppressed wheat stripe rust disease

The *Streptomyces* isolate XF with strong inhibitory activity against *Pst* urediniospores was isolated from the peony rhizosphere soil collected in Yangling, Shaanxi, China. Light microscopy revealed abnormal germination of urediniospores treated with various dilutions of XF fermentation filtrate (FL) (Additional file 1: Figure S1). Among them, urediniospores treated with the original FL (1×) failed to germinate (Additional file 1: Figure S1), which translates into an inhibition rate of 99.17% (Fig. 1a). The 100-fold dilution of FL (100×) showed antagonistic activity against urediniospore with a 69.68% germination rate, which was considerably lower than the blank control (CK) (Fig. 1a). Meanwhile, the original FL showed a lethality rate of 61.47% against urediniospores, while triadimefon (Tr) was 95.78% (Additional file 1: Figure S2b, c). Electron microscopy results showed that most urediniospores remained non-germinated on wheat leaves sprayed with FL and Tr (Additional file 1: Figure S2d). These results suggest that FL has strong inhibitory effects against *Pst* urediniospores.

The actinomycete cell suspension (AC, 10^7 CFU/mL, Additional file 1: Figure S3) and the original FL were used to spray 14-day-old seedlings in the pot inoculation experiments. As shown in Additional file 1: Figure S4a, b, in the control treatment, *Pst* inoculated leaves were chlorotic and covered with urediniospores, whereas urediniospores were only observed sporadically on leaves of plants in the treated groups. XF AC and FL treatments significantly decreased the stripe rust disease indices (Fig. 1b) and resulted in disease control efficiencies being 65.48% and 68.25%, respectively (Fig. 1c).

In field trials, wheat leaves spray-inoculated with sterile distilled water (SDW), Tr, and XF fermentation broth (XF) on April 21 and April 26, respectively, and the incidence of wheat stripe rust was investigated two weeks later. The results showed that plants in control groups were moderately susceptible, with abundant urediniospores and no tissue necrosis. Wheat treated with XF appeared more resistant, with lower levels of sporulation
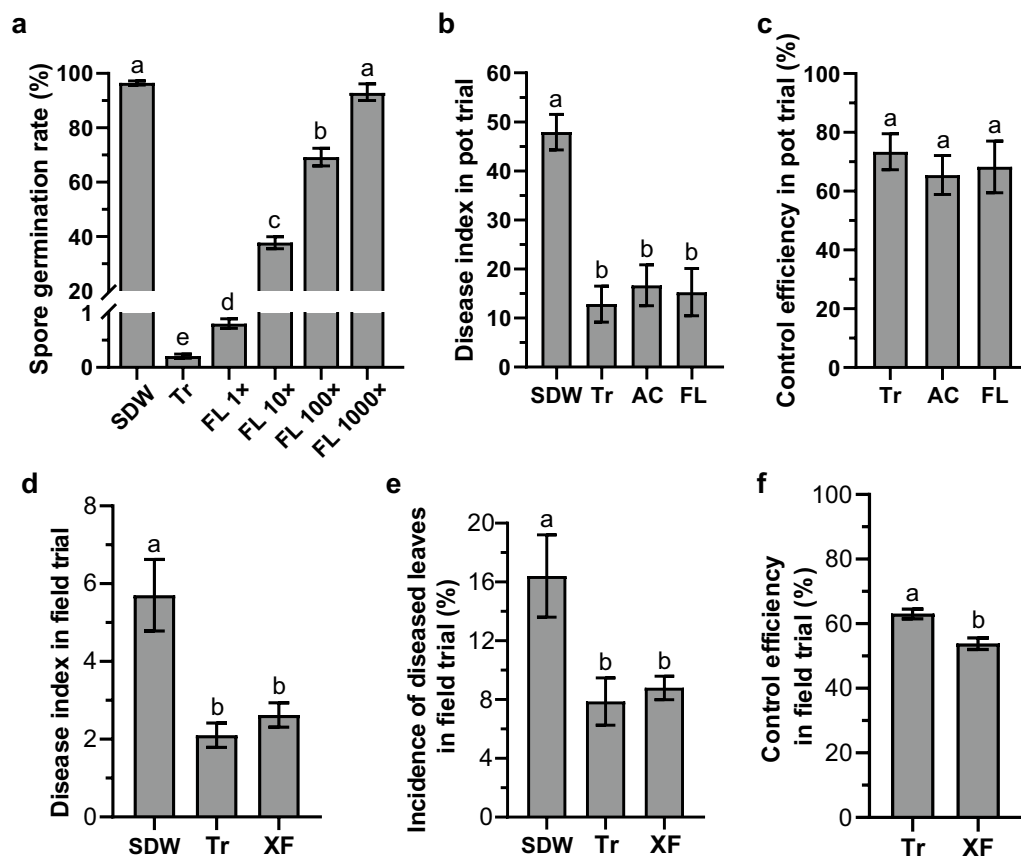
Jia *et al. Phytopathology Research*   (2023) 5:14

Page 3 of 16

Fig. 1 The control effect of *Streptomyces tauricus* XF on wheat stripe rust. **a** The germination rate of urediniospores treated with various dilutions of fermentation liquid. SDW, sterile distilled water; Tr, triadimefon was 20 μg/mL; FL, XF fermentation filtrate; ' × ' represents the dilution factor. **b** The disease index in a pot trial. Tr, 20% triadimefon emulsions at a concentration of 0.5 g/L. **c** Control efficiency of XF against wheat stripe rust in a pot trial. The three values were not significantly different from each other. **d** The disease index of wheat stripe rust in the field trial. **e** Wheat leaves disease incidence in the field trial. **f** The control efficiency in the field trial. SDW, sterile distilled water; AC, XF actinomycete cell suspension (10⁷ CFU/mL); FL, XF fermentation filtrate; XF, XF fermentation broth containing AC and FL. Values in charts are mean ± SD. By Duncan's new multiple range tests, different lowercase letters indicate differences with significance level 0.05

and chlorotic stripes on the leaves (Additional file 1: Figure S4c, d). Overall, the disease indices and incidence of diseased leaves in the plots treated with XF were significantly lower than in the control treatment (Fig. 1d, e). Strain XF elicited a biocontrol efficacy of 53.83% against stripe rust (Fig. 1f).

Characterization and identification of the strain XF
Strain XF exhibited typical morphological characteristics of the genus *Streptomyces*. The XF colony had a hard texture and a wrinkled surface with white aerial mycelia and light pink spores on Gause's Medium (GM) (Fig. 2a). Different spore masses were present on various agar plates (Additional file 1: Figure S5c). The details of the XF cultural characteristics are shown in Additional file 2: Table S1. Moreover, scanning electron microscopy (SEM) photos revealed the morphology of long filamentous rods

of the XF hyphae and the presence of cylindrical spores, forming a flexuous spore chain with a rough surface (Fig. 2b). Biochemical tests indicated that XF was able to use all the tested carbon and nitrogen sources (Additional file 1: Figure S5a, b and Additional file 2: Table S2). Extracellular enzymatic activity assays revealed that strain XF could secret several hydrolytic enzymes, including amylase, cellulase, and protease (Additional file 1: Figure S5d). Additionally, XF was able to grow at low temperatures (Additional file 1: Figure S5e). Although its growth rate slowed with decreasing temperature, it maintained viability at 9℃ and 16℃, the culture conditions for *Pst*.

To observe the colonization of XF on leaves at low temperature, AC (1 × 10⁷ CFU/mL) were spray-inoculated onto wheat leaves. Electron microscopy shows the XF growth in wheat leaves treated with AC for 5 days at 16℃ (Additional file 1: Figure S6). We observed a mass
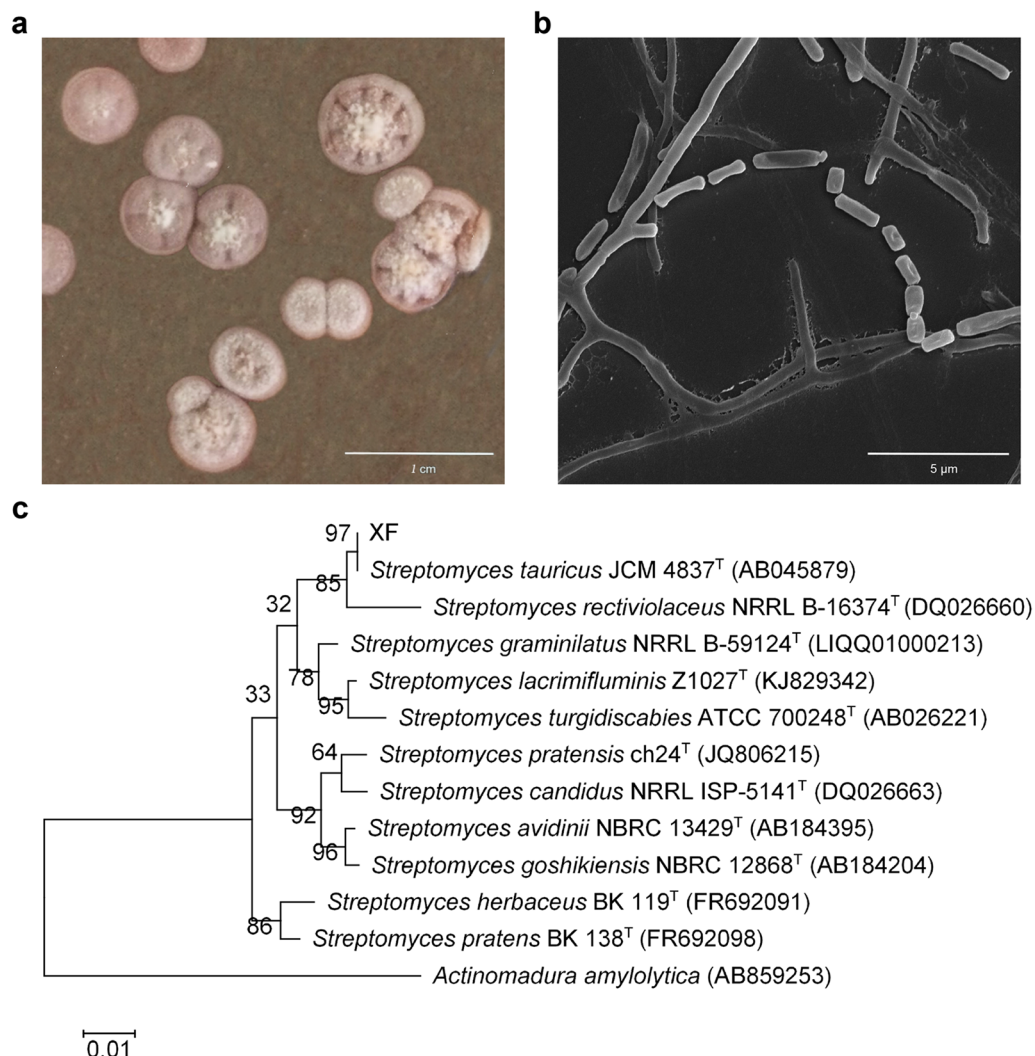
Fig. 2 Identification of XF. **a** The morphological feature of XF on Gause's Medium (GM). Bar = 1 cm. **b** Scanning electron microscope photo of XF spore chain. Bar = 5 μm. **c** Phylogenetic tree based on the partial nucleotide sequence of 16S RNA genes. Numbers between segments represent bootstrap support values, and 'T' above represents the strain as a model strain

of superficial mycelia covering the leaf surfaces (Additional file 1: Figure S6b), and some appeared to grow into the stomatal openings (Additional file 1: Figure S6c) and substomatal cavities (Additional file 1: Figure S6d). These results indicate that XF could grow on wheat leaves.

To confirm the phylogenetic relationship between XF with *Streptomyces* species, we amplified the 16S rRNA sequences of XF and conducted sequence alignments in the EzTaxon-e server. The original 16S rDNA sequencing data were available in the NCBI SRA database with the accession number OM541329. Analysis of the 16S rRNA sequence demonstrated that XF matches *S. tauricus* JCM 4837 (AB045879) at 99.65% and that XF and *S. tauricus* clustered in one phylogenic group (Fig. 2c). These results confirm that strain XF is an isolate of *S. tauricus*.

Strain XF inhibited *Pst* growth in leaves

The primary leaves of 14-day-old wheat were inoculated with 20 μL fresh urediniospores of *Pst* (3×10^4 spores/mL). The AC (10^7 CFU/mL) and FL of XF was sprayed onto the wheat leaves 24 h before *Pst* inoculation, respectively. Leaves were then harvested at 36 and 72 hours post-inoculation (hpi) of XF, and the fungal structures were stained with wheat germ agglutinin (WGA). The results showed that the infected area, hyphal length, and haustoria of *Pst* at 36 hpi and 72 hpi on AC- and FL-treated leaves were considerably lower than those in control (SDW) (Fig. 3a–d). In particular, haustorium formation rates was reduced more significantly at 72 hpi comparison with at 36 hpi (Fig. 3d). Meanwhile, the effects of AC and FL treatments were comparable to those of the Tr treatment. These observations
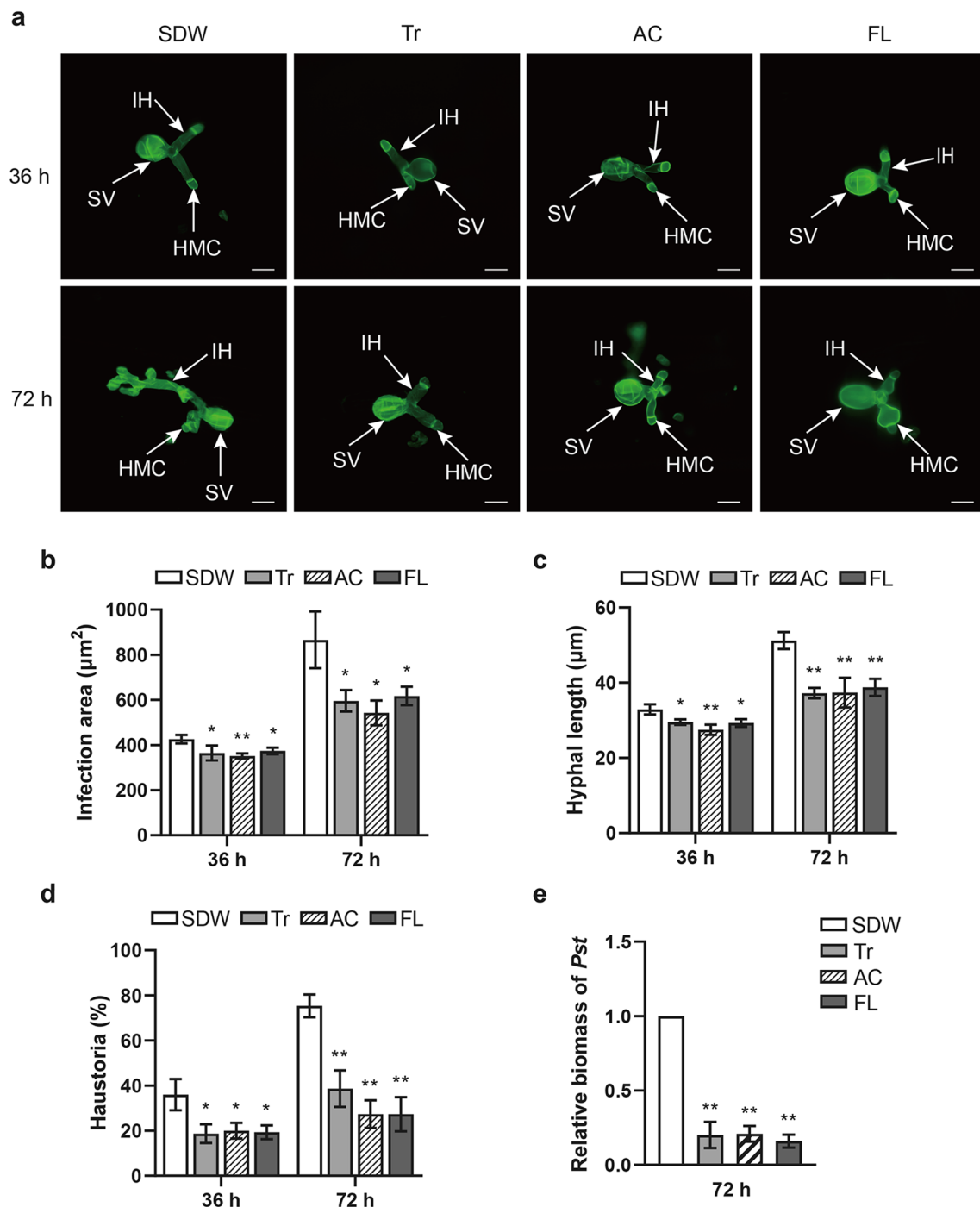
Fig. 3 Effects of XF on *Pst* growth in leaves. **a** Histological observation of fungal growth in wheat. SV, substomatal vesicle; IH, infectious hyphae; HMC, haustorial mother cell. Bars = 20 μm. **b** Infection area, the average area of the expanding hypha plus the host cells, was calculated by CellSens Entry software. **c** Hyphal length is the average distance from the junction of the substomatal vesicle and the hypha to the tip of the hypha. **d** Haustoria formation rate of *Pst* with various treatments. **e** RT-qPCR analysis of the relative expression levels of *PstEF* in leaves at 72 h after inoculation with Tr, AC, and FL. *TaEF* and *PstEF* were used to normalize the RNA level of wheat leaves and *Pst*, respectively. SDW, sterile distilled water; Tr, 20% triadimefon emulsions at a concentration of 0.5 g/L; AC, XF actinomycete cell suspension (10^7 CFU/mL); FL, XF fermentation liquid without actinomycete cells. Values in charts are mean ± SD. An asterisk indicates significant differences based on the unpaired two-tailed Student's *t*-test with the *P* values marked (*$P < 0.05$; **$P < 0.01$) between the SDW treatment and other treatments

Jia *et al. Phytopathology Research*   (2023) 5:14

Page 6 of 16

demonstrated that AC and FL strongly reduced the *Pst* infection areas, hyphal lengths, and haustorium formation rates. In addition, the *Pst* biomass in wheat was also significantly reduced at 72 h after treatment with AC and FL (Fig. 3e). Thus, we conclude that strain XF limits *Pst* expansion in wheat leaves.

Strain XF promoted ROS burst in wheat leaves and reduced *Pst* infection rates

To further define the repressive role of XF on *Pst*, fourteen-day-old wheat were inoculated with AC and FL, and maintained under normal growth conditions for 24 h, then inoculated with *Pst*. Leaves were collected at 36 hpi

and 72 hpi of XF, and DAB staining were performed to detect the reactive oxygen species (ROS) area and stripe rust infection. After *Pst* infection, ROS accumulation were observed in Tr, AC, and FL treatment (Fig. 4a). The ROS areas in the AC and FL treatments were considerably more significant than the water control at 36 h and 72 h (Fig. 4a, b), indicating that AC and FL promoted ROS bursts in wheat leaves (Fig. 4). The infection rates of *Pst* were lowered more by XF compared to SDW, as shown in Fig. 4c. AC treatments resulted in significantly lower infection rates than SDW treatments, 1.83% at 36 h and 2.29% at 72 h. At 36 h, FL had a strong inhibitory effect on *Pst* infection with only a 3.90% infection rate.
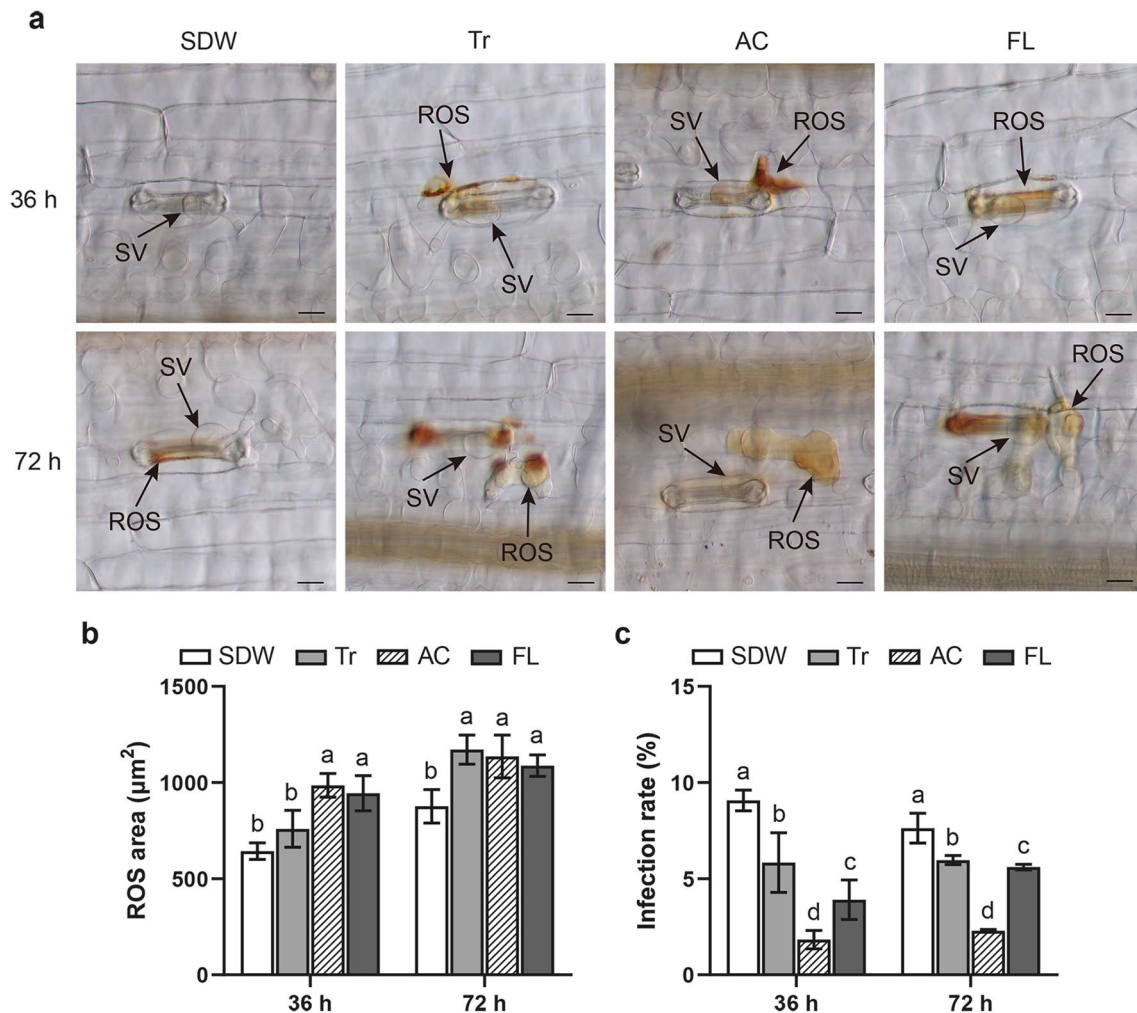

Fig. 4 Effects of XF treatments on ROS production and infection rate of *Pst* on wheat leaves. **a** Histological observation of H_2O_2 accumulation after DAB staining in wheat leaves. SV, substomatal vesicle. Bars = 20 μm. **b**, **c** The ROS area of wheat leaves (**b**) and the infection rate of *Pst* (**c**) in the various treatment groups. Only infection sites where substomatal vesicles had formed over stomata were considered successful infections and were microscopically observed for the presence or absence of haustoria. The infection rate was calculated as the number of penetration sites that exhibited one or multiple haustoria in relation to the total number of stomata. Values in the chart are mean ± SD. By Duncan's new multiple range tests, different lowercase letters indicate differences with significance level 0.05

Jia *et al. Phytopathology Research* (2023) 5:14

Page 7 of 16

Strain XF induced the expression of defense-related genes in wheat leaves

To determine whether the XF strain could induce disease resistance in wheat, the first true leaf of '2 leaves and 1 heart' wheat was sprayed with FL and AC (10^7 CFU/mL) and the second true leaves were collected at 12, 18, 24, 36, 42, 48, 72, and 120 hpi of XF. The transcript levels of genes encoding phenylalanine ammonia-lyase (*PAL*) and pathogenesis-related (*PR*) proteins, including antifungal protein (*PR1*), β-1,3-endoglucanases (*PR2*), chitinases (*PR3*), endochitinase (*PR4*), and peroxidase (*PR9*) were analyzed. As shown in Fig. 5, six genes were upregulated to varying degrees at different time points except for the 18 hpi. Salicylic acid (SA)-related genes *PR1*, *PR2*, and *PAL* showed maximum expression at 120 hpi in FL-treated plants, with a fold change of 134.18, 38.04, and 3.24, respectively, compared to the control (Fig. 5 and Additional file 1: Figure S7). However, the peak of relative expression of *PR1* and *PR2* in AC-treated plants appeared

at 12 hpi, with 7.30- and 7.97-fold change, respectively. These results indicated that the expression of gene *PR1* and *PR2* were mainly activated by AC at the early stage of inoculation, while FL mainly induced the expression of the two genes in the late stage. Additionally, with the jasmonic acid (JA)/ ethylene (ET)-related genes *PR3*, *PR4*, and *PR9*, the overall dynamics of *PR3* expression were similar to those with *PR4* expression (Fig. 5). Expression levels of the two genes in the FL-treated group were all higher than those in the AC-treated group at 12, 42, 48, and 120 hpi. Remarkably, the relative expressions of gene *PR3* and *PR4* both reached a maximum at 120 hpi, and the expression of *PR4* in the FL-treated group was ten-fold higher than in the AC-treated group at this time (Additional file 1: Figure S8a, b). For the gene *PR9*, wheat treated with AC or FL, the gene was significantly up-regulated at all time points compared to the control group, except for 18 hpi and 36 hpi (Fig. 5). Gene expression peaked at 48 h in both AC- and FL-treated groups, with
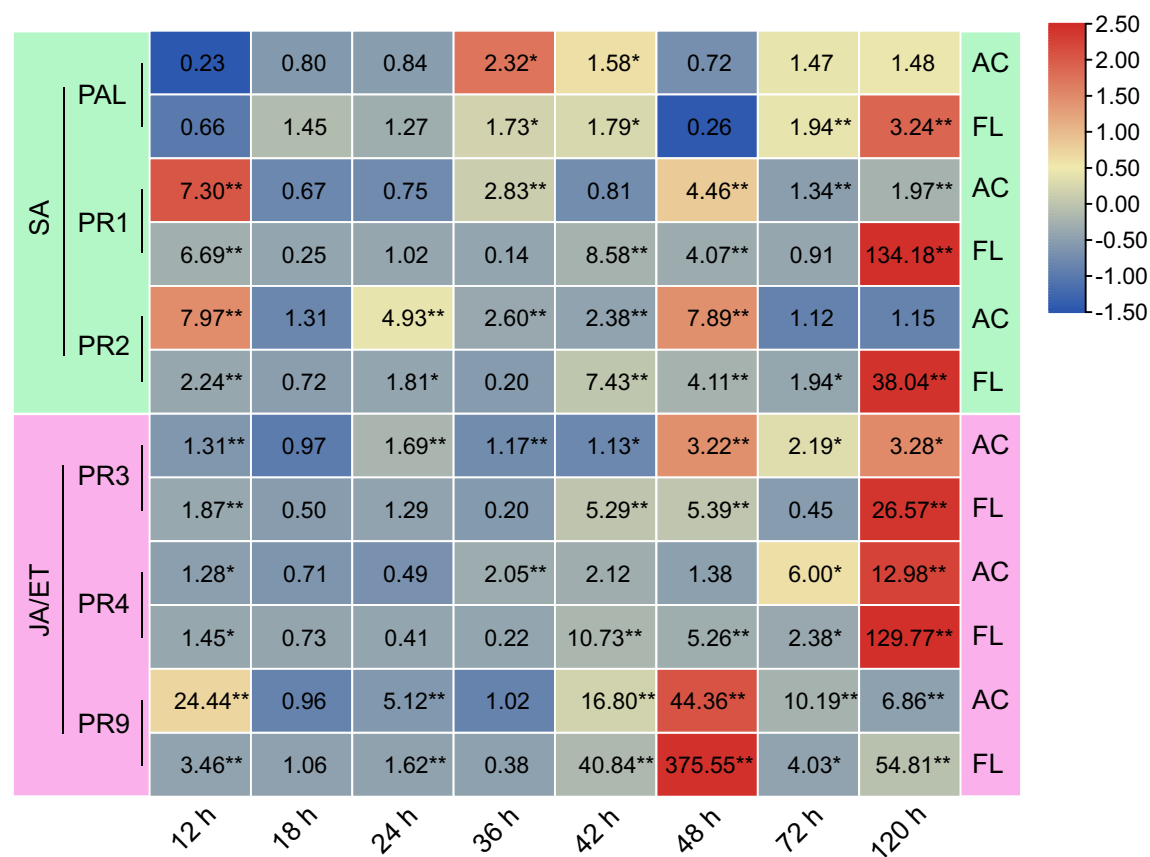

Fig. 5 Expression of defense-related genes in wheat leaves induced by XF. The first true leaf of wheat was sprayed with fermentation filtrate (FL) and actinomycete cell suspension (AC), and the second true leaves were collected at 12, 18, 24, 36, 42, 48, 72, and 120 hours post-inoculation (hpi) of XF. The horizontal axis in heat maps represents different time points, and each square shows the relative transcript levels of each gene in the AC or FL treatment. The heatmap was row-normalized using the scale method. The higher the gene expression, the hotter (redder) the color. An asterisk indicates significant differences based on the unpaired two-tailed Student's *t*-test with the *P* values marked (**P* < 0.05; ***P* < 0.01) between treatments and the sterile distilled water (SDW) control, and only significantly up-regulated expressions are marked in the figure

Jia *et al. Phytopathology Research*   (2023) 5:14

Page 8 of 16

44.36- and 375.55-fold increases (Additional file 1: Figure S8c), respectively.

The ethyl acetate extracts of FL exhibited antagonistic activity against urediniospores

To obtain the active ingredients, XF FL was extracted sequentially using petroleum ether (PE), dichloromethane (DCM), ethyl acetate (EA), n-butanol (NB), and the remaining portion (R) was concentrated. The EA phase of FL had the highest *Pst* antifungal activity and the urediniospores germination rate was reduced to 0.66% (Additional file 1: Figure S9). Thus, subsequent tests were conducted with EA as an extraction solvent, and the ethyl acetate phase active substance (EAP) was obtained by extraction with EA. After extraction of the FL with EA, the remaining aqueous fraction were concentrated in vacuo to obtain the non-ethyl acetate phase active substance (NEAP). Consistent with the results above, as shown in Additional file 1: Figure S10, the EAP active substance exhibited a much stronger antagonistic effect than the NEAP. The germination rates of urediniospores treated with NEAP were only 16.82%, whereas the EAP-treated urediniospores failed to germinate (Additional file 1: Figure S10), which translates into an inhibition rate of 99.90%, and proteinase K (proE K) treatment did not affect the inhibitory activity of the extracts (Fig. 6a and Additional file 1: Figure S10). These results indicate that the active substance reducing urediniospore germination in XF FL is probably not a protein(s) but a chemical or combination of chemicals with polarity similar to the EA.

To confirm the inhibitory effect of EAP extracts on *Pst*, the antifungal activities of EAP at various concentrations were evaluated by testing the urediniospore germination and *Pst* mortality rates. The inhibition rate of urediniospore germination was 18.29% at 25 mg/L, but increased significantly to 86.12% at 50 mg/L (Fig. 6b). The inhibitory effect of EAP on urediniospores was up to nearly 99%, similar to that of the Tr treatment, when the concentration was increased to over 100 mg/L. As shown in Fig. 6c, low concentrations of EAP resulted in urediniospore cytoplasm release and germ tube swelling and deformation, accompanied by much shortened germ tube than observed in the SDW treatment. The results of the survival tests showed that EAP treatment resulted in the death of urediniospores (Fig. 7a). The mortality rate increased with increasing EAP concentrations and duration of treatments, and eventually reached 25%, which was much higher than the SDW treatments but still far less than the Tr-treated group (Fig. 7b).

Discussion

Using microorganisms to control plant disease is a sustainable alternative to conventional fungicides (Araujo 2022). The ability of *Streptomyces* species to produce plant-protective substances, such as enzymes, secondary metabolites, and volatile organic compounds, as well as their ability to induce plant immunity to respond to pathogens rapidly, indicate that they are good candidates as biocontrol agents (Newitt et al. 2019). In this study, *S. tauricus* XF was demonstrated to effectively control wheat stripe rust and its secondary metabolites have positive roles in resistance to *Pst*. The mechanisms behind this phenomenon may be associated with multiple factors, such as direct phytopathogen suppression and inducing broad-spectrum plant disease resistance. Both mechanisms have potential applications for biological control of wheat stripe rust.

Five types of spores are produced during the stripe rust fungus life cycle; asexual urediniospores are responsible for facilitating the most damaging phase of wheat stripe rust disease (Jiao et al. 2017), and almost all biochemical and molecular studies have focused on urediniospores and their infection structures (Chen et al. 2014). Consequently, urediniospores will likely play a decisive role in developing more effective strategies for stripe rust control. Screening beneficial microorganisms for agents that can suppress urediniospores has been suggested in previously reported literature (Li et al. 2013; Zhan et al. 2014; Zheng et al. 2017) and has been confirmed in our research. The inhibition of urediniospore germination was used as an indicator to evaluate the antagonistic activity of candidate isolates against *Pst.* The strain XF stood out because of its strong inhibitory effect on urediniospores. The mortality rate of urediniospores was used as a marker for the fungicidal activity of the XF strain against stripe rust. Trypan blue staining was used to observe activities of urediniospores during interaction between XF and *Pst* (see dark blue deactivated urediniospores in Fig. 7). Based on these observations, we believe it is possible to combine studies on the germination inhibition rate and mortality of urediniospores to screen microorganisms for bio-control potential against wheat rust more efficiently.

S. tauricus is a microorganism of great interest in the medical field by secreting various compounds with anti-cancer and anti-human pathogenic activity, but it has been less studied in agriculture. However, as early as twenty years ago, *S. tauricus* 19/97 M was found to stimulate the growth of coniferous seedlings and protect them from diseases caused by *Fusarium* and *Alternaria* fungi (Gaidasheva et al. 2022), which heralded the potential of *S. tauricus* for agricultural disease control. This potential was subsequently demonstrated in several
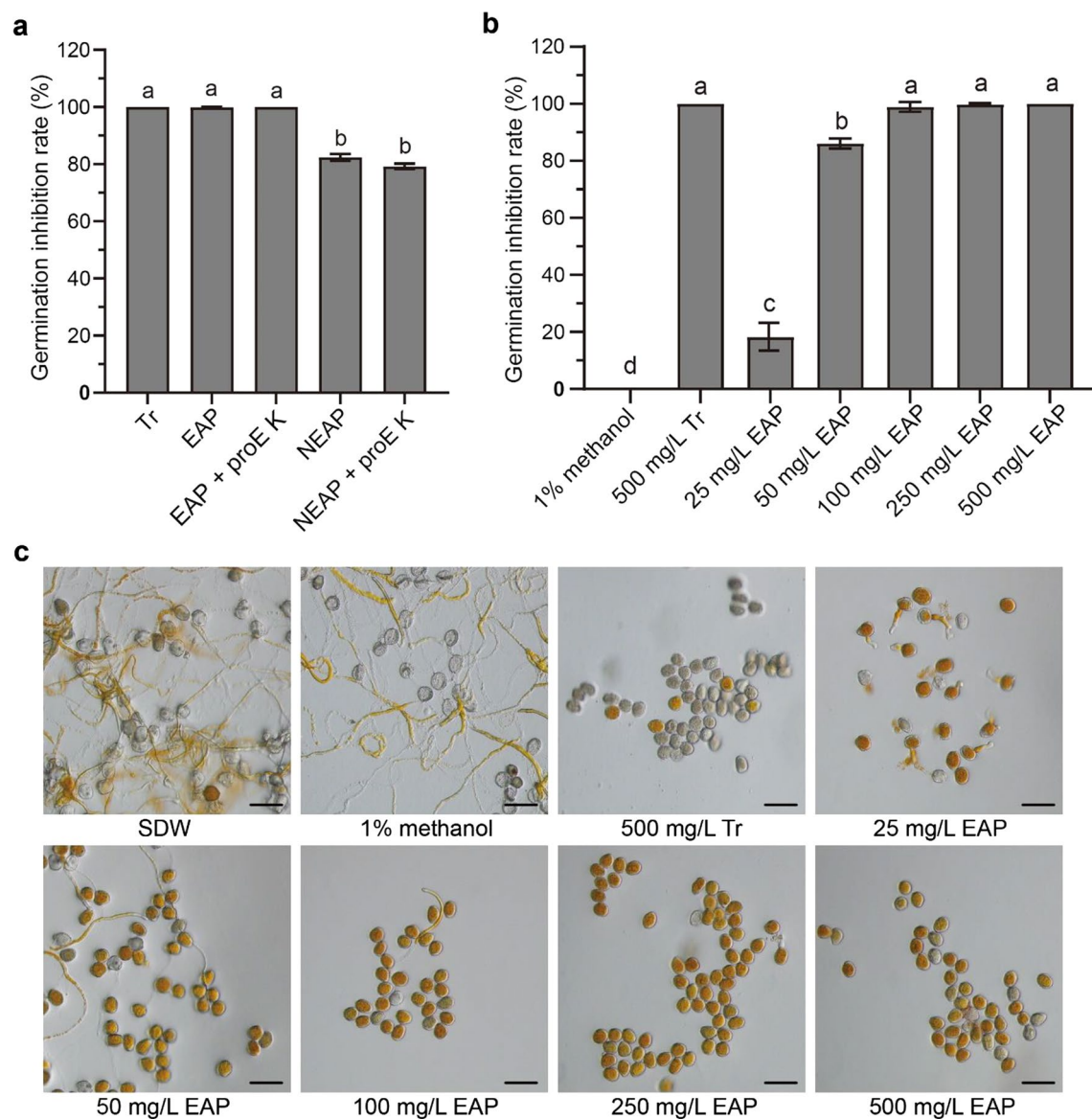
Jia *et al. Phytopathology Research*   (2023) 5:14

Page 9 of 16

Fig. 6 Effect of different concentrations of EAP solution on the germination of *Pst* urediniospores. **a** Comparison of the inhibition rate of urediniospore germination by EAP and NEAP before and after treatment with proE K. Values in the chart are mean ± SD. By Duncan's new multiple range tests, different lowercase letters indicate differences with significance level 0.05. **b** Inhibition rate of urediniospore germination by incubating with different concentrations of EAP solution for 12 h at 9℃ in the dark. **c** Morphology of urediniospores in the above treatments under the optical microscope. Bars = 50 μm. EAP, ethyl acetate phase active substance; NEAP, non-ethyl acetate phase active substance; proE K, proteinase K. Sterile distilled water (SDW), 1% methanol, and Tr were used as controls

(See figure on next page.)
Fig. 7 Mortality of ethyl acetate phase active substance (EAP) on *Pst* urediniospores. **a** Status of urediniospores after incubation at 9℃ in the dark for different times in each treatment under the optical microscope. AS, alive status; ES, emergence status; DS, death status. Bars = 50 μm. **b** Urediniospore mortality rate in the various treatment groups at each time point. Comparisons were made between different time points for the same treatment, and the values in the chart are mean ± SD. By Duncan's new multiple range tests, different lowercase letters indicate differences with significance level 0.05
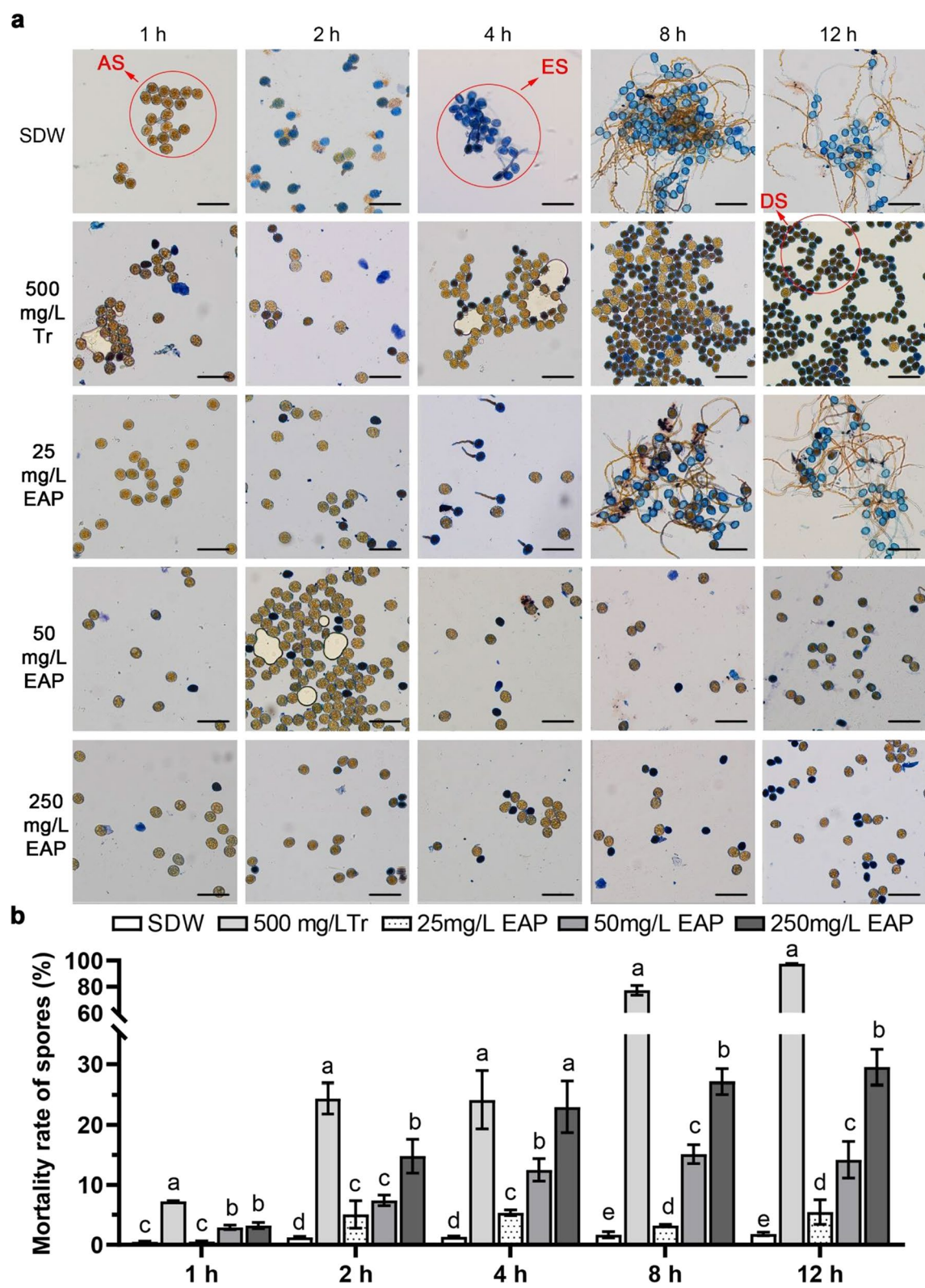
Fig. 7 (See legend on previous page.)

Jia *et al. Phytopathology Research*　　(2023) 5:14

Page 11 of 16

reports. Berg et al. (2006) found that a strain identified as *S. tauricus* isolated from strawberry rhizosphere soil could inhibit the growth of *Verticillium dahlia*, which causes yellow wilt. The *S. tauricus* JS2 strain has antagonistic activities against *Ceratocystis fimbriata*, the pathogen of pomegranate wilt, and inhibits southern root-knot nematode infestations (Zhou et al. 2016). However, studies on the effectiveness of *S. tauricus* against phytopathogenic fungi have been limited to determining inhibition activities in vitro or in greenhouse experiments (Bhai et al. 2018). There is little information in the literature about the efficiency of this genus against plant fungal diseases under field settings. In the present study, *S. tauricus* XF has high efficacy against stripe rust in greenhouse and field trials. Interestingly, XF mycelia could grow on wheat leaf surfaces and XF perform cell wall hydrolytic activities and the ability to utilize various carbon sources in plate assays. These results indicate that *S. tauricus* XF has potential for agricultural applications to control foliar disease in wheat.

Streptomyces spp. are known to be producers of antifungal compounds (Sabaratnam and Traquair 2015). Numerous studies indicate that the EAP of metabolites secreted by *Streptomyces* spp. have a broad spectrum of antifungal activities. For example, the EAP of *S. griseocarneus* was able to inhibit the growth of *F. oxysporum* f. sp. *cubense* (Jakubiec-Krzesniak et al. 2018), *Colletotrichum gloeosporioides*, and the rice pathogen *Burkholderia gladioli* (Betancur et al. 2017). The antifungal metabolites of *S. alfalfa* XN-04 were also concentrated in EAP extracts (Chen et al. 2021). In this study, the XF EAP had potent inhibitory activity against *Pst*. EAP begins to work within the first 2 h of *Pst* interactions. Although low concentrations of EAP did not affect urediniospore germination, they did impact germ tube growth by suppressing length extensions or abnormal branching (Fig. 6c), as shown in leaf observations (Fig. 3a). Higher concentrations of EAP exerted biocontrol activity by inhibiting germination and killing the urediniospores. Our findings support literature reports on the antifungal activity of *Streptomyces* spp. For instance, *S. griseocarneus* could inhibit the spore germination and mycelia growth of tomato fungal pathogens by secretion of rhizostreptin (Sabaratnam and Traquair 2015). *Streptomyces* sp. CEN26 produces 2,5-bis (hydroxymethyl) furan monoacetate, a compound that deformed conidial germination and appressorium formation of the fungal pathogen (Phuakjaiphaeo et al. 2016). It is possible that *S. tauricus* XF tested herein synthesizes extracellular antifungal compounds antagonistic to *Pst*.

An additional mechanism whereby *Streptomyces* spp. can indirectly protect plants is by activating host resistance pathways. *Streptomyces* spp. have previously been shown to activate plant defense responses generated by biotic stresses through the induction of antioxidant enzymes and improved ROS management (Singh et al. 2016). Previous studies speculated that ROS was involved in initiating resistance responses in potato tubers or by acting as an intermediate transducer of elicitor signaling (Zhao et al. 2005). In our study, the ROS areas of leaves at 24 h after XF application were significantly more extensive than SDW at 12 h and 48 h after *Pst* inoculation (Fig. 4), indicating that XF enhances ROS generation in wheat. We speculate that increased defense responses occurred after XF inoculation. *Streptomyces* spp. have also been shown to induce the expression of defense associated genes in plants (Vurukonda et al. 2018). Gene *PR1* has commonly been used as a SAR activation marker, which enhances plant resistance to various pathogens (Ali et al. 2018; Jia et al. 2022). In this study, FL significantly induced *PR1* gene expression. A similar phenomenon was also reported in several other studies. For example, the fermentation broths of *Streptomyces* sp. JCK-6131 (Le et al. 2021) and *Streptomyces* sp. AgN23 (Vergnes et al. 2020) were previously reported to induce *PR1* gene expression in tomato and *Arabidopsis thaliana*. Also, strain FL and AC were able to activate the expression of the *PR3*, *PR4*, and *PR9* genes. Many studies have shown that *Streptomyces* spp. can trigger ISR by activating defense pathways dependent on either SA or JA/ET. Van Wees et al. (2008) reported that activation of the SA and JA/ET pathways resulted in enhanced protection compared with independent activation of each pathway. Indeed, priming oak roots with *Streptomyces* AcH 505 protected the trees against powdery mildew by activating both the SA and JA/ET signaling pathways (Kurth et al. 2014). In comparison, streptomycetes appeared to activate plant defense response pathways without pathogen infections (Kurth et al. 2014). However, whether the XF-induced plant disease resistance is dependent on both SA and JA signaling pathways needs to be further studied.

Conclusions

The effectiveness of the isolated *S. tauricus* strain XF in controlling the wheat stripe rust disease was investigated in this research. Strain XF FL exhibited strong antagonistic and fungicidal effects against urediniospores. In particular, the EAP of FL has been shown to possess high antifungal activity, which provides a theoretical foundation for the extraction and isolation of antimicrobial compounds in future studies. Additionally, both FL and AC have been shown to hamper *Pst* growth in leaves and enhance ROS production in wheat, which plays important roles in reducing the incidence of diseased leaves and disease index. Furthermore, XF fermentation broth appeared to reduce stripe rust development in the field.

Jia *et al. Phytopathology Research*   (2023) 5:14

Page 12 of 16

However, additional research is needed to determine how XF colonizes leaves and whether the XF colonization induces wheat disease resistance against stripe rust.

Methods
Plant material, plant pathogens, and chemical fungicide
The wheat genotype Suwon 11 and the *Pst* pathotype Chinese Yellow Rust 31 (CYR31) were used in laboratory and greenhouse experiments. Both were obtained from the Crop Disease Prediction and Management Group at Northwest A & F University (Yangling, Shaanxi Province, China). Wheat seedlings were grown in a greenhouse under 8/16 h night/day conditions at 16℃. *Pst* race CYR31 was propagated on Suwon 11 as described by Tang et al. (2015b). Fresh urediniospores were harvested from infected wheat leaves and stored at 4℃ with desiccant until used. Tr, 20% Emulsifiable Concentrate (Jiangsu Jianpai Agrochemical Co., Ltd.) at a concentration of 0.5 g/L was used as a positive control in pot trial and field trial.

Isolation of bio-control strains and preparation of formulations
The healthy peony rhizosphere soil was used to isolate and screen the potential strains for biocontrol. Healthy plant roots were collected from soil in Yangling, Shaanxi, China (108°4′9″E, 34°15′49″N), and the surface soil was gently brushed off. Rhizosphere actinomycetes were isolated using dilution plating (Awla et al. 2017). Actinomycetes colonies were chosen based on their growth rate, colony size, and morphological traits on the agar plates. Pure cultures were obtained by re-growth on GM plates and preserved as spore suspensions in 20% glycerol in a −80℃ freezer.

To obtain fermentation broth, 5 plugs ($\Phi = 6$ mm) of the isolates were placed into a 250 mL conical flask containing 100 mL liquid GM and shaken at 28℃ and 160 r/min for 7 d. After centrifuging at 10,000 *g* for 10 min, the actinomycete cells at the bottom, containing XF mycelial fragments and spores, were re-suspended with SDW and adjusted to a concentration to 10^7 CFU/mL of AC. The supernatant was filtered through a 0.22 μm sterile filter to obtain FL without actinomycete cells.

Evaluation of biocontrol efficiency
In vitro antifungal activity test
For screening strains with antagonistic effects on *Pst*, the inhibitory effect of the isolate's FL with different dilutions on *Pst* urediniospores germination was determined according to previously described (Li et al. 2013), with slight modifications. Briefly, the isolate's FL were collected and diluted with SDW to obtain a stock solution and 10-, 100-, and 1000-fold dilutions. The positive control was 20 μg/mL Tr and the negative control was SDW. Each treatment consisting of 20 mL of the above solutions was added to a 9-cm-diameter petri dish and freshly harvested urediniospores were uniformly sprinkled on the liquid surface. All treatments were incubated for 12 h at 9℃ in the dark and urediniospore germination was evaluated with a light microscope (Olmypus BX-43). A spore was considered to have germinated if the length of the germination tube was at least half the length of the spore.

For the lethality assay, the urediniospore survival status in FL solutions was investigated, with SDW as a blank control and 100 μg/mL Tr as a positive control. The assay was performed as described above and samples were kept in the dark at 9℃. After 12 h, urediniospores were collected and stained with trypan blue as previously described, with slight modifications (Swain et al. 2017). Briefly, the harvested urediniospores were stained with 0.2% trypan blue for 3 min at 25℃. The staining was observed, and spore survival rates were calculated. The experimental designs were completely randomized with three replicates for each treatment and repeated three times.

Pot assays
The biocontrol efficacy of XF against stripe rust in growth chambers was determined with the wheat cultivar Suwon 11. For the pot-based inoculation assays, 14-day-old seedlings were sprayed with FL and AC (10^7 CFU/mL), respectively, using a small air hand sprayer. The fungicide Tr (0.5 g/L) and SDW were positive and negative controls, respectively. At 24 h after treatment, the leaves were inoculated with 20 μL of *Pst* urediniospores at a concentration of 3×10^4 spores/mL suspended in the e-fluoride solution. The inoculated seedlings were held below dew point humidity conditions at 10℃ in the dark for 24 h, and then moved to the greenhouse regimen at 16℃. Three pots each with 9 wheat seedlings were used for each treatment, and the experiments were repeated three times. After 14 d of incubation in the growth chamber, the severity (S) of the wheat stripe rust infections was recorded. Based on the percentages of the leaf areas covered by urediniospores, the number of diseased leaves were recorded at all levels and the incidence (I), average severity ($\overline{S}$), disease index (DI), and control effects (CE) were calculated as follows:

$$I(\%) = \frac{\text{number of diseased leaves}}{\text{number of investigated leaves}} \times 100\%$$

$$\overline{S}(\%) = \frac{\sum_{i=1}^{n}(X_i \cdot S_i)}{\sum_{i=1}^{n} X_i} \times 100$$

Jia *et al. Phytopathology Research*   (2023) 5:14

Page 13 of 16

$$DI = \frac{\sum_{i=0}^{n}(X_i \cdot S_i)}{\sum_{i=0}^{n}(X \cdot S_{max})} \times 100$$

$$CE_{treatment}(\%) = \frac{DI_{control} - DI_{treatment}}{DI_{control}} \times 100\%$$

Severity was classified at 1 to 8 levels corresponding to a coverage of 1, 5, 10, 20, 40, 60, 80, and 100% according to the percentage of leaf areas covered by the urediniospores. i indicates the disease grade, X_i consists of the number of leaves with disease grade i, S_i is the value of disease grade i; X represents the total number of investigated leaves, while S_{max} shows the highest severity grade; *treatment* indicates different treatments, *control* indicates blank control, $CE_{treatment}$ is the control efficiency of different treatments (These classifications are defined by NY/T 1443.2–2007, the agricultural industry standard of the People's Republic of China).

Field trials
Wheat cultivar Mingxian 169 was planted for field experiments at Caoxin Village, Yangling, Shaanxi Province in China, during the 2021–2022 growth season. The field trials were conducted using a randomized plot design with three replicates for each treatment. Each plot was 5 m^2 in size with 20 cm spaces between the rows and 20 cm between the plots. Seeds were sown on October 23, 2021, and the field was managed using conventional practices in the region. At elongation stage of wheat with no rust uredia observed, treatments of XF fermentation broth and Tr were applied on 21st and 26th of April 2022. Strain XF fermentation broth containing actinomycete cells and fermentation filtrate was used, and the Tr was applied at a 0.5 g/L concentration. SDW was a negative control. Each plot was sprayed with 600 mL each of the above solutions. On May 11, 2022, 250 leaves were surveyed in each plot, and the incidence and severity of wheat stripe rust under each treatment was recorded.

Identification and characterization of XF
Morphological and cultural characterizations
Morphological characterizations were conducted by SEM (Hitachi model S-3400N, Japan). The cultural characteristics of XF, including color of spore mass, aerial mycelium, substrate mycelium, and diffusible pigments, were recorded after incubation at 28°C for 7 days on TSA, YMS, 2CMY, AS-1, ISP3, ISP4, and MS media (Kieser et al. 2000), and ingredients of culture media are in the Additional file 2: Table S3.

Phylogenetic analyses
The forward primer (5′-ATGCCATTCGTGCGGAGG TTG-3′) and the reverse primer (5′-CGTCTCTGC TGTCATCACTTCGTAT-3′) were used for 16S rRNA sequence amplification (Zhang et al. 2021). The amplifying procedure followed the method described by Jangir et al. (2018), and the amplified 16S rRNA fragments were sequenced (Qingke, Xi'an, China), and submitted to the EzTaxon-e server (http://www.ezbiocloud.net/) for comparative analysis. Phylogenetic trees were constructed with MEGA 7.0 software using the Maximum Likelihood method with 1000 bootstrap replications (Kumar et al. 2015).

Strain characterizations
According to the *Manual of Common Bacterial System Identification*, six different carbon substrates (sucrose, rhamnose, mannitol, lactose, glucose, and xylose) and the nitrogen sources (Ca (NO$_3$)$_2$, KNO$_3$, NaNO$_3$, NH$_4$Cl, NH$_4$NO$_3$, and glutamate) were used to substitute for the original carbon and nitrogen sources resulting in a final carbon source concentration of 1% and a nitrogen source concentration of 0.5%. The XF strain was inoculated on medium plates with different carbon and nitrogen sources, with the nitrogen source basal medium and the carbon source basal medium serving as controls. The characteristics of the colony mycelium, and the colony color were observed after 7 days of incubation at 28°C. To test XF growth at low temperatures, AC were inoculated onto GM plates and incubated separately at 9°C, 16°C, and 28°C. Mycelial growth was recorded on the 5th day after inoculation. In addition, XF was examined qualitatively for the production of extracellular enzymes, including protease, cellulase, and amylase, according to previous protocols (Hu et al. 2022).

ROS staining and measurements of infection rate
H$_2$O$_2$ accumulation was detected by staining leaves with 3, 3′-diaminobenzidine (DAB) (Xu et al. 2019). Briefly, leaves collected 36 h and 72 h after XF inoculation were treated in DAB buffer under light for 8 h. Following absorption of the DAB solution, leaves were destained in the solution (absolute ethyl alcohol: acetic acid, 1:1 v/v) and then immersed in chloral hydrate until they became clear. Only infection sites in which substomatal vesicles had formed were considered successful penetrations. A total of 60 infection sites per treatment were observed with Bright-field microscopy, and the ROS area was calculated using CellSens Entry software. The infestation rate of *Pst* was calculated as the number of the infected sites (20) divided by the total number of stomata evaluated (N) according to the method with minor modifications (Tang et al. 2015a). The assay was repeated three times.

Jia *et al. Phytopathology Research*   (2023) 5:14

Page 14 of 16

Histological observation of fungal growth

Sampled leaves were fixed and stained as previously described (Tang et al. 2015b) until the samples became transparent. After incubation in 2.0 mL of 1 M KOH in a boiling water bath for 30 min, the leaves were rinsed three times with 50 mM Tris–HCl (pH 7.4) for 15 min and incubated in WGA Alexa488 solution (cat. no. W11261, Thermo Fisher Scientific). Fifty infection sites were observed with an Olympus BX-51 microscope. The infected areas, hyphal lengths, and haustorial mother cells were observed and used for CellSens Entry software (version: V1.7) calculations.

Scanning electron microscopy

Sampled leaves were treated for SEM examination as described by (Li et al. 2013). *Pst* growth in leaves was observed using a Nano SEM-450. Leaves were collected and treated for SEM as described. The observation of XF growth on leaves was performed following the above description.

RNA extraction and reverse transcription-quantitative PCR (RT-qPCR) analysis

Total RNA of the harvested leaves was extracted with Trizol and converted to cDNA using the PrimeScript™ RT reagent Kit with gDNA Eraser following the manufacturer's protocols. Biomass quantification was performed as described by Xu et al. (2019), and the biomass of wheat and *Pst* was determined by the internal reference genes *TaEF* (wheat elongation factor 1 alpha) and *PstEF* (rust elongation factor 1). In addition, the expression of SA- (*PR1*, *PR2*, and *PAL*) and JA/ET-related genes (*PR3*, *PR4*, and *PR9*) in leaves were determined, and the *TaEF* gene was used as the internal control gene. All primer sequences are shown in Additional file 2: Table S4. RT-qPCR was performed using UltraSYBR Mixture (CWBIO, China). Each treatment contained three independent biological replicates, and each replicate contained three technical replicates. Relative transcript levels were calculated using the $2^{-\Delta\Delta CT}$ method (Livak and Schmittgen 2001).

Preparation of crude extracts

Four solvents, PE, DCM, EA, and NB, were used sequentially in a polar gradient approach to define the polarity range of active substances in XF FL (Chen et al. 2021). Specifically, we extracted 100 mL of FL with an equivalent volume of PE overnight. After incubation, the solution was separated into two layers, and the target phase was collected and concentrated with a vacuum concentrator. The remaining phase was extracted overnight with an equivalent volume of DCM. In subsequent procedures, we recovered the PE, DCM, EA, NB, and R

extracts. All extracts were dissolved in 0.5% methanol to 50 mg/L and used for antifungal activity assay.

XF FL was extracted with an equal volume of EA overnight. Following full extraction, the mixture was separated into two layers. The EA upper layer was then evaporated using rotary evaporator to yield the EAP. The lower aqueous solution was collected and dried to obtain NEAP. These fractions were dissolved in 100 mL of 0.5% methanol, and stored at 4°C. In addition, protein was removed by incubating 5 mL of EAP and NEAP for 1 h at 37°C with 25 µl of proE K (10 mg/mL, already pre-treated at 58°C for 2 h).

Data processing

All data are presented as mean values ± standard deviation (SD). Data were subjected to analysis of variance (ANOVA) followed by Duncan's multiple range tests using SPSS11.0 (SPSS Inc., Chicago, IL, USA).

Abbreviations

AC	Actinomycete cell suspension
BCAs	Biocontrol agents
CYR31	Chinese Yellow Rust 31
DAB	3, 3′-Diamino benzidine
EAP	Ethyl acetate phase
ET	Ethylene
FL	Fermentation filtrate
HMC	Haustorial mother cell
hpi	Hours post-inoculation
IH	Infectious hyphae
ISR	Induced system resistance
JA	Jasmonic acid
NEAP	Non-ethyl acetate phase active substance
PAL	Phenylalanine ammonia-lyase
PR	Pathogenesis related
proE K	Proteinase K
Pst	*Puccinia striiformis* F. sp. *tritici*
ROS	Reactive oxygen species
SA	Salicylic acid
SDW	Sterile distilled water
SEM	Scanning electron microscopy
SV	Substomatal vesicle
Tr	Triadimefon
WGA	Wheat germ agglutinin

Supplementary Information

The online version contains supplementary material available at https://doi.org/10.1186/s42483-023-00168-y.

Additional file 1. Figure S1. Effects of different dilutions of XF fermentation filtrate (FL) on *Pst* urediniospores germination. **Figure S2**. Antagonistic effect of XF fermentation filtrate (FL) on *Pst* uredospores. **Figure S3**. Colony growth of XF on Gause's Medium (GM) plates. **Figure S4**. Biocontrol efficacy of XF against wheat stripe rust in a growth chamber and in a field trial. **Figure S5**. The cultural characteristics of XF. **Figure S6**. Leaf surfaces of the XF AC-treated seedlings observed by scanning electron microscope. **Figure S7**. Expression of SA-responsive pathogenesis-related genes in wheat leaves induced by XF. **Figure S8**. Expression of JA/ET-responsive pathogenesis-related genes in wheat leaves induced by XF. **Figure S9**. Antagonistic effect of extracts of different solvents on *Pst* urediniospores. **Figure S10**. Effect of EAP and NEAP of XF on uredniospore germination and their stability to protease.

Jia *et al. Phytopathology Research*   (2023) 5:14

Page 15 of 16

Acknowledgements

Authors' contributions

YW, RJ, and KX designed the study. RJ, KX, LY, and LH performed the experiments. RJ, KX, LY, and JC analysed data. RJ, KX, and YW wrote the manuscript. All authors read and approved the final manuscript.

Funding

Availability of data and materials

Not applicable.

Declarations

Ethics approval and consent to participate

Not applicable.

Consent for publication

Not applicable.

Competing interests

The authors declare that they have no competing interests.

References

Ali S, Ganai BA, Kamili AN, Bhat AA, Mir ZA, Bhat JA, et al. Pathogenesis-related proteins and peptides as promising tools for engineering plants with multiple stress tolerance. Microbiol Res. 2018;212–213:29–37. https://doi.org/10.1016/j.micres.2018.04.008.

Araujo R. Advances in soil engineering: sustainable strategies for rhizosphere and bulk soil microbiome enrichment. Front Biosci. 2022;27:195. https://doi.org/10.31083/j.fbl2706195.

Araujo R, Dunlap C, Barnett S, Franco CMM. Decoding wheat endosphere-rhizosphere microbiomes in rhizoctonia solani-infested soils challenged by *Streptomyces* biocontrol agents. Front Plant Sci. 2019;10:1038. https://doi.org/10.3389/fpls.2019.01038.

Awla HK, Kadir J, Othman R, Rashid TS, Hamid S, Wong MY. Plant growth-promoting abilities and biocontrol efficacy of *Streptomyces* sp. UPMRS4 against *Pyricularia oryzae*. Biol Control. 2017;112:55–63. https://doi.org/10.1016/j.biocontrol.2017.05.011.

Beddow JM, Pardey PG, Chai Y, Hurley TM, Kriticos DJ, Braun HJ, et al. Research investment implications of shifts in the global geography of wheat stripe rust. Nat Plants. 2015;1:15132. https://doi.org/10.1038/nplants.2015.132.

Berg G, Opelt K, Zachow C, Lottmann J, Gotz M, Costa R, et al. The rhizosphere effect on bacteria antagonistic towards the pathogenic fungus *Verticillium* differs depending on plant species and site. FEMS Microbiol Ecol. 2006;56:250–61. https://doi.org/10.1111/j.1574-6941.2005.00025.x.

Betancur LA, Naranjo-Gaybor SJ, Vinchira-Villarraga DM, Moreno-Sarmiento NC, Maldonado LA, Suarez-Moreno ZR, et al. Marine *Actinobacteria* as a source of compounds for phytopathogen control: an integrative metabolic-profiling/bioactivity and taxonomical approach. PLoS ONE. 2017;12:e0170148. https://doi.org/10.1371/journal.pone.0170148.

Bhai R, Subila K, Eapen S, Reshma A, Pervez R, Bhat AI, et al. Effect of biocontrol agents on production of rooted back pepper cutting in serpentine method. J Spices Aromat Crops. 2018;27:59–65. https://doi.org/10.25081/josac.2018.v27.i1.1016.

Chen J, Hu L, Chen N, Jia R, Ma Q, Wang Y. The biocontrol and plant growth-promoting properties of *Streptomyces alfalfae* XN-04 revealed by functional and genomic analysis. Front Microbiol. 2021;12:745766. https://doi.org/10.3389/fmicb.2021.745766.

Chen W, Wellings C, Chen X, Kang Z, Liu T. Wheat stripe (yellow) rust caused by *Puccinia striiformis* f. sp. *tritici*. Mol Plant Pathol. 2014;15:433–46. https://doi.org/10.1111/mpp.12116.

Diaz-Cruz GA, Liu J, Tahlan K, Bignell DRD. Nigericin and geldanamycin are phytotoxic specialized metabolites produced by the plant pathogen *Streptomyces* sp. 11–1-2. Microbiol Spectr. 2022;10:e0231421. https://doi.org/10.1128/spectrum.02314-21.

Gaidasheva II, Shashkova TL, Orlovskaya IA, Gromovykh TI. Biosafety analysis of metabolites of *Streptomyces tauricus* strain 19/97 M, promising for the production of biological products. Bioengineering. 2022. https://doi.org/10.3390/bioengineering9030113.

Gupta R, Saxena RK, Chaturvedi P, Virdi JS. Chitinase production by *Streptomyces viridificans*: its potential in fungal cell wall lysis. J Appl Bacteriol. 1995;78:378–83. https://doi.org/10.1111/j.1365-2672.1995.tb03421.x.

Han DJ, Wang QL, Chen XM, Zeng QD, Wu JH, Xue WB, et al. Emerging YR26-virulent races of *Puccinia striiformis* f. *tritici* are threatening wheat production in the Sichuan Basin, China. Plant Dis. 2015;99:754–60. https://doi.org/10.1094/PDIS-08-14-0865-RE.

Han X, Wang J, Liu L, Shen F, Meng Q, Li X, et al. Correction for Han et al., "Identification and predictions regarding the biosynthesis pathway of polyene macrolides produced by *Streptomyces roseoflavus* Men-myco-93-63". Appl Environ Microbiol. 2021;87:e0080221. https://doi.org/10.1128/AEM.00802-21.

Jakubiec-Krzesniak K, Rajnisz-Mateusiak A, Guspiel A, Ziemska J, Solecka J. Secondary metabolites of actinomycetes and their antibacterial, antifungal and antiviral properties. Pol J Microbiol. 2018;67:259–72. https://doi.org/10.21307/pjm-2018-048.

Jangir M, Pathak R, Sharma S, Sharma S. Biocontrol mechanisms of *Bacillus* sp., isolated from tomato rhizosphere, against *Fusarium oxysporum* f. sp. lycopersici. Biol Control. 2018;123:60–70. https://doi.org/10.1016/j.biocontrol.2018.04.018.

Jia R, Chen J, Hu L, Liu X, Xiao K, Wang Y. *Alcaligenes faecalis* Juj3 alleviates *Plasmodiophora brassicae* stress to cabbage *via* promoting growth and inducing resistance. Front Sustain Food Syst. 2022. https://doi.org/10.3389/fsufs.2022.942409.

Jiao M, Tan C, Wang L, Guo J, Zhang H, Kang Z, et al. Basidiospores of *Puccinia striiformis* f. sp. *tritici* succeed to infect barberry, while urediniospores are blocked by non-host resistance. Protoplasma. 2017;254:2237–46. https://doi.org/10.1007/s00709-017-1114-z.

Kiani T, Mehboob F, Hyder MZ, Zainy Z, Xu L, Huang L, et al. Control of stripe rust of wheat using indigenous endophytic bacteria at seedling and adult plant stage. Sci Rep. 2021;11:14473. https://doi.org/10.1038/s41598-021-93939-6.

Kieser T, Bibb MJ, Buttner MJ, Chater KF, Hopwood DA, Charter K, et al. Practical *Streptomyces* genetics. John Innes Foundation: Norwich; 2000. https://doi.org/10.1111/j.1365-2427.2007.01876.x.

Kumar S, Stecher G, Tamura K. MEGA7: Molecular evolutionary genetics analysis version 7.0 for bigger datasets. Mol Biol Evol. 2015;33:1870–4. https://doi.org/10.1093/molbev/msw054.

Kurth F, Mailander S, Bonn M, Feldhahn L, Herrmann S, Grosse I, et al. Streptomyces-induced resistance against oak powdery mildew involves host plant responses in defense, photosynthesis, and secondary metabolism pathways. Mol Plant Microbe Interact. 2014;27:891–900. https://doi.org/10.1094/MPMI-13-0296-R.

Le KD, Kim J, Nguyen HT, Yu NH, Park AR, Lee CW, et al. *Streptomyces* sp. JCK-6131 protects plants against bacterial and fungal diseases via two mechanisms. Front Plant Sci. 2021;12:726266. https://doi.org/10.3389/fpls.2021.726266.

Lehr NA, Schrey SD, Hampp R, Tarkka MT. Root inoculation with a forest soil streptomycete leads to locally and systemically increased resistance against phytopathogens in Norway spruce. New Phytol. 2008;177:965–76. https://doi.org/10.1111/j.1469-8137.2007.02322.x.

Li H, Zhao J, Feng H, Huang LL, Kang ZS. Biological control of wheat stripe rust by an endophytic *Bacillus subtilis* strain E1R-j in greenhouse and field

Jia *et al. Phytopathology Research*   (2023) 5:14

Page 16 of 16

trials. Crop Prot. 2013;43:201–6. https://doi.org/10.1016/j.cropro.2012.09.008.

Hu LF, Jia RM, Sun Y, Chen J, Zhang J, Wang Y. *Streptomyces pratensis* S10 controls of fusarium head blight by suppressing different stages of the life cycle and ATP production. Plant Dis. 2022. https://doi.org/10.1094/PDIS-09-22-2063-RE.

Livak KJ, Schmittgen T. Analysis of relative gene expression data using real-time quantitative PCR and the 2-DDCt method. Methods. 2001;25:402–8.

Lucas JA, Hawkins NJ, Fraaije BA. The evolution of fungicide resistance. Adv Appl Microbiol. 2015;90:29–92. https://doi.org/10.1016/bs.aambs.2014.09.001.

Newitt JT, Prudence SMM, Hutchings MI, Worsley SF. Biocontrol of cereal crop diseases using *Streptomycetes*. Pathogens. 2019;8:78. https://doi.org/10.3390/pathogens8020078.

O'Sullivan CA, Roper MM, Myers CA, Thatcher LF. Developing actinobacterial endophytes as biocontrol products for *Fusarium pseudograminearum* in wheat. Front Bioeng Biotech. 2021;9:691770. https://doi.org/10.3389/fbioe.2021.691770.

Patel JK, Madaan S, Archana G. Antibiotic producing endophytic *Streptomyces* spp. colonize above-ground plant parts and promote shoot growth in multiple healthy and pathogen-challenged cereal crops. Microbiol Res. 2018;215:36–45. https://doi.org/10.1016/j.micres.2018.06.003.

Phuakjaiphaeo C, Chang CI, Ruangwong O, Kunasakdakul K. Isolation and identification of an antifungal compound from endophytic *Streptomyces* sp. CEN26 active against *Alternaria brassicicola*. Lett Appl Microbiol. 2016;63:38–44. https://doi.org/10.1111/lam.12582.

Sabaratnam S, Traquair JA. Mechanism of antagonism by *Streptomyces griseocarneus* (strain Di944) against fungal pathogens of greenhouse-grown tomato transplants. Can J Plant Pathol. 2015;37:197–211. https://doi.org/10.1080/07060661.2015.1039062.

Schwessinger B. Fundamental wheat stripe rust research in the 21(st) century. New Phytol. 2017;213:1625–31. https://doi.org/10.1111/nph.14159.

Singh SP, Gupta R, Gaur R, Srivastava AK. *Streptomyces* spp. alleviate *Rhizoctonia solani*-mediated oxidative stress in *Solanum lycopersicon*. Ann Appl Biol. 2016;168:232–42. https://doi.org/10.1111/aab.12259.

Sub YY, Kim SH, Kim MW, Choi GJ, Cho KY, Song JK, et al. Notes : Antifungal activity of *Streptomyces* sp. against *Puccinia recondite* causing wheat leaf rust. J Microbiol Biotech. 2004;14:422–5.

Swain DM, Yadav SK, Tyagi I, Kumar R, Kumar R, Ghosh S, et al. A prophage tail-like protein is deployed by *Burkholderia bacteria* to feed on fungi. Nat Commun. 2017;8:404. https://doi.org/10.1038/s41467-017-00529-0.

Tang C, Deng L, Chang D, Chen S, Wang X, Kang Z. TaADF3, an actin-depolymerizing factor, negatively modulates wheat resistance against *Puccinia striiformis*. Front Plant Sci. 2015a;6:1214. https://doi.org/10.3389/fpls.2015.01214.

Tang C, Wei J, Han Q, Liu R, Duan X, Fu Y, et al. PsANT, the adenine nucleotide translocase of *Puccinia striiformis*, promotes cell death and fungal growth. Sci Rep. 2015b;5:11241. https://doi.org/10.1038/srep11241.

Van Wees SC, Van der Ent S, Pieterse CM. Plant immune responses triggered by beneficial microbes. Curr Opin Plant Biol. 2008;11:443–8. https://doi.org/10.1016/j.pbi.2008.05.005.

Vergnes S, Gayrard D, Veyssiere M, Toulotte J, Martinez Y, Dumont V, et al. Phyllosphere colonization by a soil *Streptomyces* sp. promotes plant defense responses against fungal infection. Mol Plant Microbe Interact. 2020;33:223–34. https://doi.org/10.1094/MPMI-05-19-0142-R.

Vurukonda S, Giovanardi D, Stefani E. Plant growth promoting and biocontrol activity of *Streptomyces* spp. as endophytes. Int J Mol Sci. 2018;19:952. https://doi.org/10.3390/ijms19040952.

Xu Q, Tang C, Wang X, Sun S, Zhao J, Kang Z, et al. An effector protein of the wheat stripe rust fungus targets chloroplasts and suppresses chloroplast function. Nat Commun. 2019;10:5571. https://doi.org/10.1038/s41467-019-13487-6.

Ye X, Li J, Cheng Y, Yao F, Long L, Yu C, et al. Genome-wide association study of resistance to stripe rust (*Puccinia striiformis* f. sp. *tritici*) in Sichuan wheat. BMC Plant Biol. 2019;19:147. https://doi.org/10.1186/s12870-019-1764-4.

Zhan G, Tian Y, Wang F, Chen X, Guo J, Jiao M, et al. A novel fungal hyperparasite of *Puccinia striiformis* f. sp. *tritici*, the causal agent of wheat stripe rust. PLoS ONE. 2014;9:e111484. https://doi.org/10.1371/journal.pone.0111484.

Zhang J, Chen J, Hu L, Jia R, Ma Q, Tang J, et al. Antagonistic action of *Streptomyces pratensis* S10 on *Fusarium graminearum* and its complete genome sequence. Environ Microbiol. 2021;23:1925–40. https://doi.org/10.1111/1462-2920.15282.

Zhao J, Davis LC, Verpoorte R. Elicitor signal transduction leading to production of plant secondary metabolites. Biotechnol Adv. 2005;23:283–333. https://doi.org/10.1016/j.biotechadv.2005.01.003.

Zheng L, Zhao J, Liang X, Zhan G, Jiang S, Kang Z. Identification of a novel *Alternaria alternata* strain able to hyperparasitize *Puccinia striiformis* f. sp. *tritici*, the causal agent of wheat stripe rust. Front Microbiol. 2017;8:71. https://doi.org/10.3389/fmicb.2017.00071.

Zhou YL, Yuan SJ, Pan YM, Hu XQ. Studies on the toxicity of Actinomycete JS2 to pomegranate wilt pathogen and root knot nematode. Acta Agr U Jiangxiensis. 2016;38:268–74. https://doi.org/10.13836/j.jjau.2016038. (**in Chinese**).